Characterisation of WC–12Co thermal spray powders and HPHVOF wear resistant coatings

H. L. de Villiers Lovelock, J. Kinds, and P. M. Young

Fourteen commonly used, commercially available, WC 12Co thermal spray powders were characterised in terms of their particle size distribution, surface morphology, cross-sectional morphology, and phase composition. Based on the results, four powders were selected for the deposition of thermal spray coatings using the JP 5000 high pressure high velocity oxyfuel (HPHVOF) system. Dry sand rubber wheel abrasion tests were performed on the coatings in order to determine the effect of powder manufacturing method on the wear rates. The coating produced using the cast and crushed powder did not deposit well and wore through very rapidly. The abrasion tests on the remaining coatings showed that the other two powder manufacturing routes are essentially equivalent in terms of the resultant coating wear resistance.

PM/0777

At the time the work was carried out the authors were in the Thermal Spray and Repair Group of MATTEK, CSIR, PO Box 395, Pretoria 0001, South Africa. Mr Kinds is currently at the University of Groningen, 9714 AV Groningen, The Netherlands. Manuscript received 14 November 1997; in final form 30 June 1998.

INTRODUCTION

Carbide based coatings are some of the most widely utilised thermal spray coating types. They are used mainly to protect components against sliding, abrasion, fretting, and erosive wear at temperatures below 550°C.

The high pressure high velocity oxyfuel (HPHVOF) thermal spray process lends itself particularly well to the spraying of dense and well bonded WC based coatings owing to the low temperatures (about 3000°C), relative to the plasma spray process, and the high particle velocities (about 500 m s^{-1}) which are obtained,[1] hence minimising the loss of WC during the spraying process. Loss of WC is a well known phenomenon in thermal spraying and occurs primarily by a combination of decarburisation and dissolution in the binder metal during spraying, during which the WC–Co transforms to phases such as W_2C, Co_3W_3C (η phases), Co_6W_6C (ε phase), WC_{1-x}, WO_3, and W.[2–8] The original cobalt binder phase of the powder is also often replaced in the coating by an amorphous or nanocrystalline binder phase. The amorphous matrix usually contains W Co C phases such as Co_3W_3C, Co_6W_6C, $Co_3W_9C_4$, Co_2W_4C, and $Co_2W_4C_4$. These phases are not detectable by X-ray diffraction (XRD) owing to their nanocrystalline state,[2–8] but evidence of partial recrystallisation of the amorphous binder phase by means of nucleation of $Co_xW_yC_z$ crystallites at the WC/Co interface has been documented.[3,4] The amorphous Co–W–C binder alloy has also been observed to recrystallise into $Co_xW_yC_z$ phases detectable by XRD, during vacuum or air heat treatment at 900–1100 K.[5–7]

The formation of non-WC carbide phases is generally considered detrimental to the wear performance,[9–17] although it appears that in some cases the integrity of the microstructure and the intersplat cohesion can affect the wear rate more than the degree of loss of WC.[4]

The WC–Co thermal spray coating properties are affected by a large number of deposition variables, of which one of the most important is usually the powder type, and hence it was expected that this would also be the case for the HPHVOF process. Fourteen HVOF grade WC–Co spray powders were evaluated in the first part of this work. Based on the results, four powders were selected for producing coatings for wear testing.

EXPERIMENTAL PROCEDURE

Powder selection

Fifteen powders were originally selected from commercially available WC–12Co thermal spray powders. The selection was partly based on the authors' industrial job shop experience with the JP 5000 HPHVOF system. One powder was not available for testing, as indicated in Table 1. Note that the nominal sizes given in all of the tables in the present paper are not necessarily those under which the powder is marketed, but have been defined by the authors using uniform criteria, so that meaningful comparisons between powders are possible.

Particle size distribution

Although an abbreviated particle size distribution analysis is usually supplied along with the powders, a meaningful comparison can only be made if the size distribution analysis has been carried out using the same method for all of the powders. The Malvern Mastersizer laser light scattering method was used to compare the powders. The principle of this method is that a small (~5 g) powder sample is dispersed in water and circulated through a measuring cell where it is intercepted by a beam of laser light. The powder particles scatter the light in a way that is dependent on the particle size and the instrument can be calibrated accordingly. From the intensity of the various diffraction rings, the particle size distribution can then be determined. Although the absolute value of the results is often not reliable, since the method tends to be affected by particle shape and will often overestimate the percentage of coarse particles in a powder (cf. Table 3), it is extremely accurate for the detection of differences between powder samples, particularly when the powders have a similar particle shape.

Particle morphology

The surface and cross-sectional morphology of the powders was evaluated using scanning electron microscopy (SEM). Wherever possible, the average size of the WC grains within the powder particles was estimated in cross-section, using a semiquantitative graphical line drawing method as

described by Exner *et al.*[18] This could not be done for some of the powders owing to the poor separation between the WC grains in the cross-sectional image. Where appropriate, the backscattered electron mode was used in SEM in order to highlight the WC grains. When using backscattered electrons in the SEM, the WC appears brighter than the cobalt matrix, owing to the higher atomic weight of W. The method used does not distinguish between WC and other carbides, such as W_2C. For all of the powders, except some of the cast and crushed ones, almost all of the carbide grains visible in the powders were WC, as will be seen from the phase composition.

Essentially, the method consists of drawing a grid of straight gauge lines of different lengths l_T across an enlarged micrograph of a powder particle, and determining the number of WC grains N intersected by the total length of the lines $\Sigma l_T = L_T$, as well as the total portion of this length $\Sigma l_{WC} = L_{WC}$ which falls within the WC grains. If one includes enough grains in the measurement, the mean linear WC grain size $\bar{L}_{WC}$ is equal to L_{WC}/N, i.e. the total length of the line portion which finds itself in the carbide phase, divided by the number of grains making up that length of line, equals the average carbide size.

Since the average WC size varies dramatically between the different powder types, it was decided to keep N more or less constant (typically between 90 and 110), in order to try and keep the error more or less constant for each powder type. The accuracy of the final results was influenced mainly by the following factors:

(i) the choice of powder particles for the measurement was not random, since many particles were unsuitable for the conducting of measurements. Therefore, the danger exists that the powder particles chosen were not entirely representative

(ii) in the sintered and crushed and in the agglomerated and densified powders, it was usually very difficult to distinguish the boundaries between carbide grains which were in close contact with each other. It was however necessary to attempt to do so, based on the assumption that during thermal spraying these carbides will be separated and behave as separate grains

(iii) the magnification used as well as the spacing between lines and the total average length of the lines, inevitably varies depending on the powder being examined, owing to geometrical and microstructural constraints

(iv) in cross-section, it is not usual to see the true 'diameter' or dimension of a grain.

The results are, to a large extent, dependent on the best judgement of the measurer and therefore, there may be some degree of systematic error involved. Also, they are not accurate in the absolute sense, although they may be in a comparative sense (*see* (iii) above). The results should therefore be seen only as a comparative estimate of the average carbide grain size.

Table 1 WC–12Co powders selected for study (trade names are used for easier identification)

Trade name	Original lot no.	Manufacturing method	Nominal size, μm
D amalloy 2003	J9004	Cast and crushed	5–30
WC–432	1	Cast and crushed	16–45
Al 1101	PP 351 96	Cast and crushed	16–45
D amalloy 2004	9600 465B	Sintered and crushed	16–38
WC–489–1	32	Sintered and crushed	16–45
Al 1172	PP-220–96	Sintered and crushed	16–45
1342V	770 004	Sintered and crushed	16–45
WC–114	71	Sintered and crushed	11–45
72F NS	9600 005B	Sintered and crushed	11–45
Amperit 516.3	16144	Sintered and crushed	11–45
AMDRY 1927	Not available	Agglomerated and densified	≈16–45
WC–616	1	Agglomerated and densified	22–45
1341P	750 029	Agglomerated and densified	16–53
Amperit 518.074	11151	Agglomerated and densified	16–53
JK 7112 (JK 112)	265 809	Agglomerated and densified	16–45

Phase composition

Crystallographic phases present in powder

X-ray diffraction (XRD) was used to determine the phases present in the powders. Copper K_α radiation was used and the samples were run from 20 to 100° (2θ), with a step size of 0·02° (2θ) and a fixed time of 2 s per step.

Carbide phase volume fraction

Initial attempts to estimate the volume fraction of carbide phase V_V(WC), using the same graphical method as described above,[18] were only partially successful. The volume fraction can be expressed as

$$V_V(\mathrm{WC}) = \frac{\bar{L}_{WC} N}{L_T V_V}$$

This estimation is subject to the same errors elaborated above and the method can not be used accurately for powders where there is significant porosity in the particles.

Subsequently, attempts were made to determine the volume fraction of carbide or binder phases using computerised image analysis. These were, however, unsuccessful owing to the porosity within the powder particles, which made it impossible to separate the binder and the carbides, except by tedious manual methods.

Finally, theoretical binder and carbide volume fractions were calculated from the chemical analysis results as supplied by the manufacturer. Under the assumption that the non-WC carbides are insignificant in the calculation, and ignoring all elements present in quantities smaller than 1%, the WC volume fraction was estimated as

$$\frac{(\text{wt-\%}[\mathrm{W}+\mathrm{C}]/\rho_{WC})}{(\text{wt-\%Co}/\rho_{Co}) + (\text{wt-\%Cr}/\rho_{Cr}) + (\text{wt-\%}[\mathrm{W}+\mathrm{C}]/\rho_{WC}) + \sum(\text{wt-\%}[M_i]/\rho_{Mi})}$$

where ρ represents the density, and M_i represents other metals, such as Fe. The following values were used for

Table 2 Spray parameters used to deposit coatings

Barrel type	Short (4 in) barrel
Combustion pressure	711–773 kPa
Oxygen supply pressure	1450 kPa
Cooling water flowrate	0·38 L min^{-1}
Kerosene (fuel) flowrate	0·35 L min^{-1}
O_2 flow	4·7 × 10^{-4} m^3 min^{-1}
Spray distance and angle	380 mm, 90°
Powder feeder	Miller Rotofeed 1270
Powder feedrate and approx. wheel speed	88 g min^{-1}, 5·5 rev min^{-1}
Powder carrier gas	26 L min^{-1}
Gun traverse speed	375 mm s^{-1}
Pass step size	5 mm

Table 3 Particle size analysis results for all three powder types

Powder	% passing 45 μm sieve	Nominal size	5% smaller than, μm	10% smaller than, μm	50% smaller than, μm	90% smaller than, μm
Cast and crushed						
Diamalloy 2003	100	5–30	5·5	7·4	16·2	30·5
WC–432	99	16–45	15·0	17·3	31·1	55·3
AI 1101	99	16–45	13·8	17·9	32·7	53·1
Sintered and crushed						
Diamalloy 2004	88	16–38	12·5	16·1	27·4	44·7
WC–489–1	98	16–45	16·5	19·7	33·8	55·4
AI 1172	99	16–45	11·6	16·5	33·5	57·0
1342V	95	16–45	16·6	20·2	34·2	57·2
WC 114	99	11–45	11·4	14·6	28·9	50·2
72F NS	96	11–45	12	14·4	31·3	54·8
Amperit 516.3	99	11–45	11·2	15·7	31·3	51·4
Agglomerated and densified						
WC·616	98	22–45	20·5	23·6	35·6	53·5
1341P	92	16–53	15·2	18·8	35·8	60·7
Amperit 518.074	98	16–53	18·2	21·3	36·0	61·5
JK 7112 (JK 112)	95	16–45	15·5	19·4	35·2	55·9

the densities: $\rho_{Co} = 8{\cdot}9$ g cm^{-3}, $\rho_{Cr} = 7{\cdot}2$ g cm^{-3}, $\rho_{WC} = 15{\cdot}7$ g cm^{-3}, $\rho_{Fe} = 7{\cdot}9$ g cm^{-3}.

The calculation is based on the assumption that all of the carbon is present in the form of WC, which is not strictly correct but is essentially unavoidable unless the free carbon content is known. The effect of other carbides should be negligible since their densities are not radically different from that of WC ($\rho_{W_2C} \approx 17{\cdot}1$ g cm^{-3}), and they are present in small quantities, as will be seen below.

Since the carbide fraction is not considered of primary importance, bearing in mind that all of the powders are of similar composition, no further attempts were made to measure the carbide fraction.

Coating deposition

Four powders, namely Praxair WC–432, Praxair WC–489–1, Metco 72F NS, and Praxair WC–616 were selected on the basis of the results of the powder evaluation. Using these powders, coatings were produced using the spray parameters listed in Table 2.

Microstructural characterisation and microhardness testing

The coatings produced were sectioned using a Struers Unitom cutting machine with a low cutting feedrate, mounted in cold setting resin, and ground and polished using a semiautomatic polishing machine (Struers Rotopol/Pedemat). The coating microstructures were evaluated in cross-section using optical microscopy. Low porosity and carbide pullout after preparation (the latter indicating insufficient bonding of the carbides in the matrix), the presence of well distributed retained carbide particles, and the absence of large binder 'pools' were regarded as the most important attributes when comparing the coatings. Microhardness testing was done using a Leitz tester with a load of 0·3 kg. The average of 10 indentations was taken. Care was taken not to situate the indentations near the coating edge, near pores, or near each other, to within eight indentation diameter lengths.

Abrasion resistance

The coatings produced were tested in dry sand rubber wheel three body abrasion tests. In this test, a flat specimen is pressed against a rotating rubber wheel while sand is fed into the interface between the specimen and the wheel. The apparatus and method used correspond to ASTM G65–94, except that a lower load (50 N) was applied to the specimen/wheel interface, and rounded Delmas silica of size 5–350 μm instead of angular Ottawa silica of size 210–300 μm was utilised. Specimens were weighed at 5 min intervals and the total testing time was 25 min. The wheel speed was 200 rev min^{-1} and the diameter 227·5 mm. As is usual for this test, the wear rates were initially high and became reasonably stable after 5–10 min. Each result is an average of two specimens tested.

EXPERIMENTAL RESULTS

Particle size distribution

The Malvern particle size analysis results are shown in Table 3 along with selected sieve analysis results supplied by the powder manufacturers. Based on the authors' experience with the HPHVOF system to date, those

Table 4 Average size and volume percentage of visible carbides in powders: nd = not determined

Powder	Average size, μm	Size range estimated from micrographs, μm	Visible carbide content, vol.-%	
			Chemical analysis	Graphical analysis
Cast and crushed				
Diamalloy 2003 (fine)	2·16	1–5	nd	nd
WC–432	3·09	2–12	82·2	77·2
AI 1101	3·34	2–12	81·8	55·5
Sintered and crushed				
Diamalloy 2004	nd	nd	80·1	nd
WC–489–1	1·42	0–4	80·4	81·4
AI 1172	1·64	1–6	80·8	74·3
1342V	nd	nd	79·8	nd
WC–114	1·03	0–4	80·1	80·4
72F NS	nd	0–4	80·6	nd
Amperit 516.3	1·00	0–8	80·3	66·2 (very porous)
Agglomerated and densified				
WC–616	1·36	0–5	80·6	73·9
1341P	1·55	0–6	80·7	87·3
Amperit 518.074	1·71	0–6	80·9	81·6
JK 7112 (JK 112)	1·35	0–5	80·7	not possible

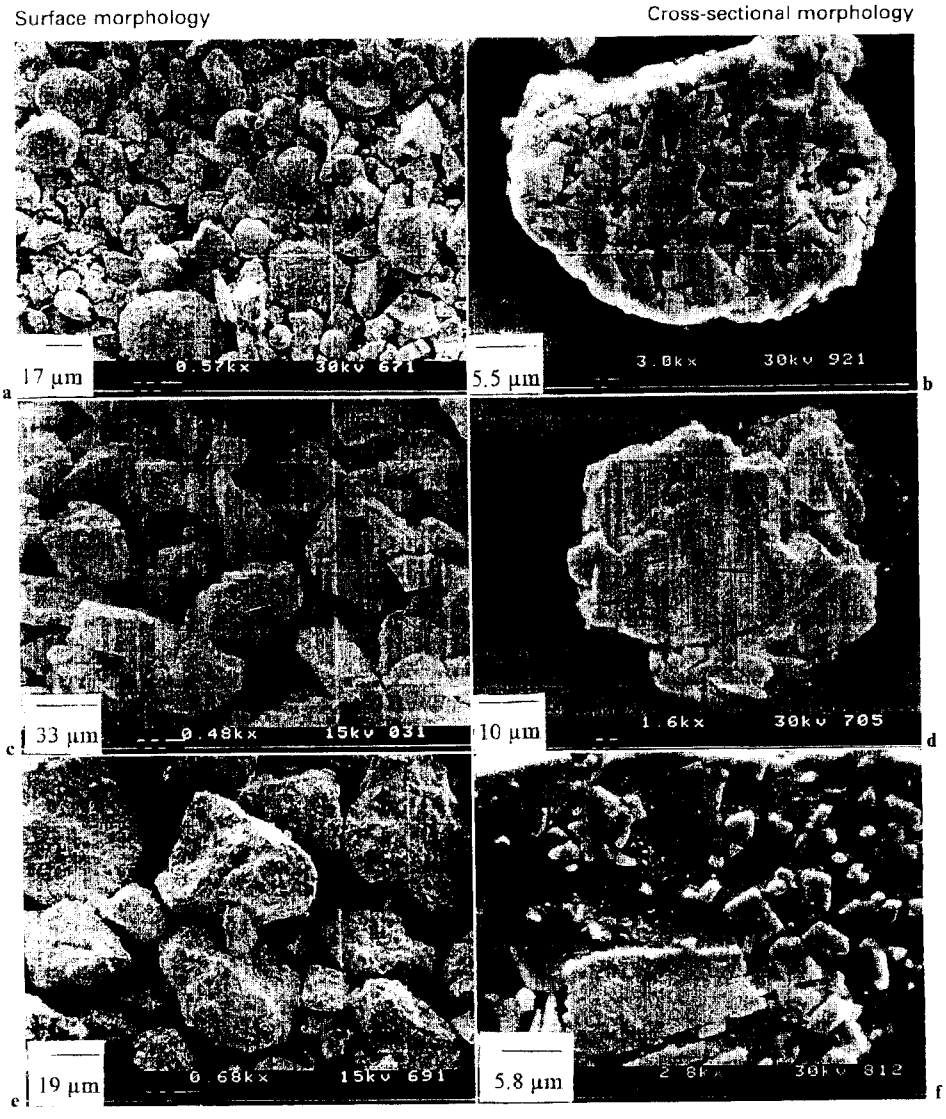

a Diamalloy 2003; *b* Diamalloy 2003; *c* WC–432; *d* WC–432 (note large WC size); *e* AI 1101; *f* AI 1101

1 Surface morphologies and cross-sections of cast and crushed powders

powders with the lowest percentage of particles below 16 μm were to be considered first for spraying trials. These are the Praxair WC–432 and AI 1101 (cast and crushed group) and Praxair WC–489–1 or TAFA 1342V (sintered and crushed group). In the agglomerated and densified group, all four powders tested were acceptable from a size range point of view.

Particle morphology

The powder surface and cross-sectional morphologies are shown in Figs. 1–3, and the results of the WC size measurements are shown in Table 4. The following observations may be made.

The average WC size in the cast and crushed powders varies between 2·16 and 3·34 μm. Praxair WC–432 and AI 1101 have the largest WC size and this is clearly seen in the cross-sections (Fig. 1*d* and *f*). The particle surface morphology of these two powders is cleaner and more regular. Hence, based on both size (cf. above) and morphology, either WC–432 or AI 1101 would be a good choice for coating trials, and the former was chosen based on availability.

The average WC size in the sintered and crushed powders varies between 1·00 and 1·64 μm. The morphologies of all the powders are similar. Based on carbide grain size, either 72F NS or AI 1172 would be selected, since it is believed that a coarser WC size may lead to less WC decomposition during the coating process. This is the opposite choice to that which would be made based only on particle size (cf. above). Hence, both 72F NS and WC–489–1 were selected from this group for coating trials, in order to see if there was any obvious effect on abrasion resistance or microstructure resulting from the differences in the starting powders.

The average WC size in the agglomerated and densified powders varies between 1·35 and 1·71 μm. The TAFA 1341P and Amperit 518.074 powders had a 'looser' particle structure than the other two powders, and the former contained particles with a wide range of shapes and densities. The JK 7112 powder had a pronounced mixture of densified and non-densified particles (in agglomerated and plasma densified powders, some non-densified particles would be expected, because not all of the particles can pass through the centre of the induction plasma during densification). Based on these observations, WC–616 and

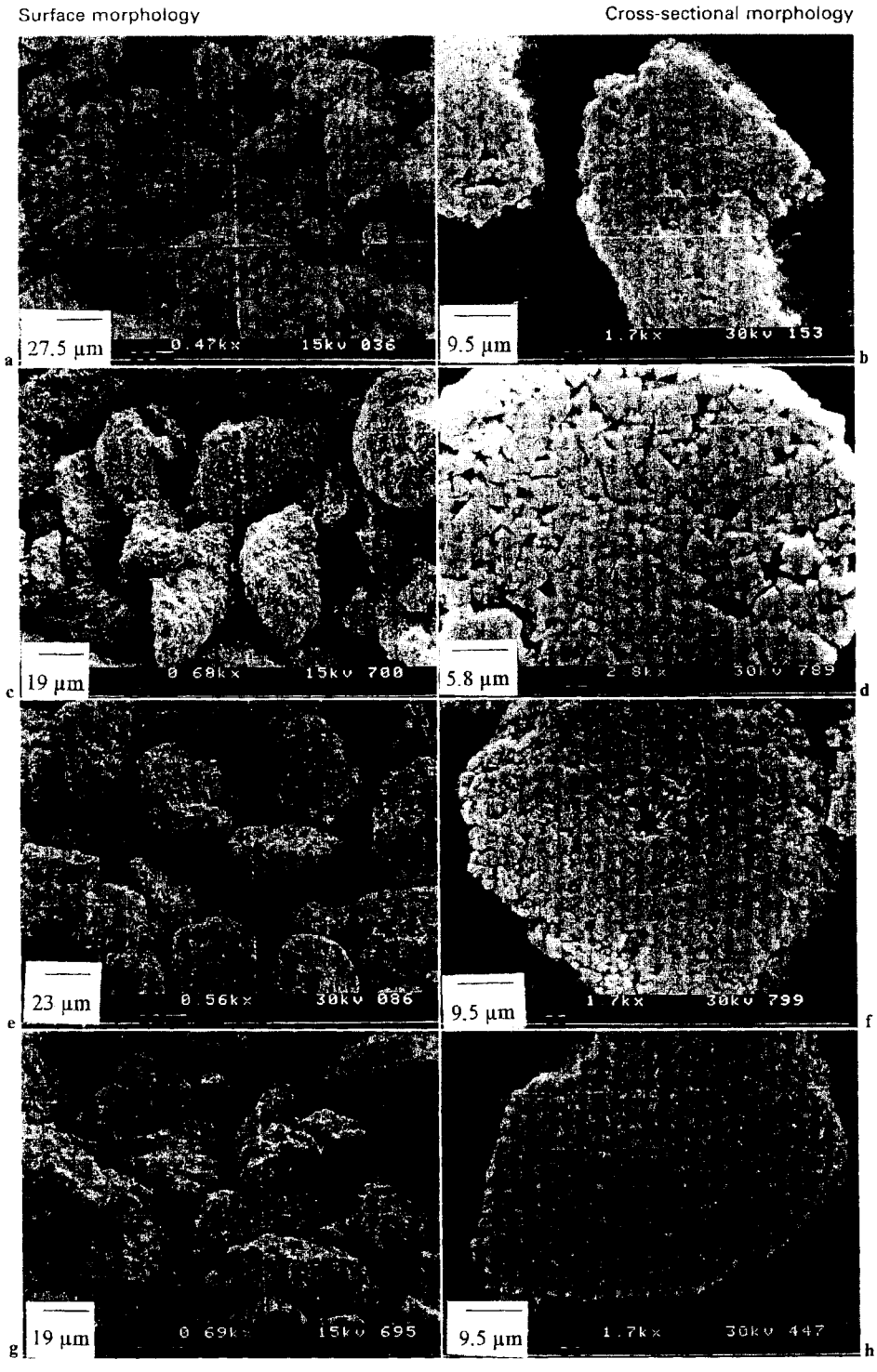

a WC–489·1 (powders 1342V, WC–114, and 72F NS all had similar morphologies); *b* WC–489–1 (powders 1342V, WC–114, and 72F NS all had similar morphologies); *c* AI 1172; *d* AI 1172; *e* 72F NS; *f* 72F NS; *g* Amperit 516.3; *h* Amperit 516.3

2 Surface morphologies and cross-sections of sintered and crushed powders

Amperit 518.074 have a more consistent morphology and would be favoured for spray trials, but since the latter is not readily available in South Africa, WC–616 was chosen.

Phase composition

Crystallographic phases present in powder

The phase compositions of the powders are summarised in Table 5. The numbers which are given indicate the ratio of the major phase peak height of each phase to the $d = 2{\cdot}518$ WC peak height, multiplied by 100. This does not represent a volume or mass percentage. The positions of the major peaks are as follows: $d = 0{\cdot}228$ nm (W_2C), $d = 0{\cdot}213$ nm (Co_3W_3C), $d = 0{\cdot}217$ nm ($Co_3W_9C_4$), $d = 0{\cdot}224$ nm (W), $d = 0{\cdot}208$ nm (CoC_x), $d = 0{\cdot}2205$ nm (Co) (hcp).

The cast and crushed powders have a greater tendency to contain W_2C and ternary W–Co–C phases, as would

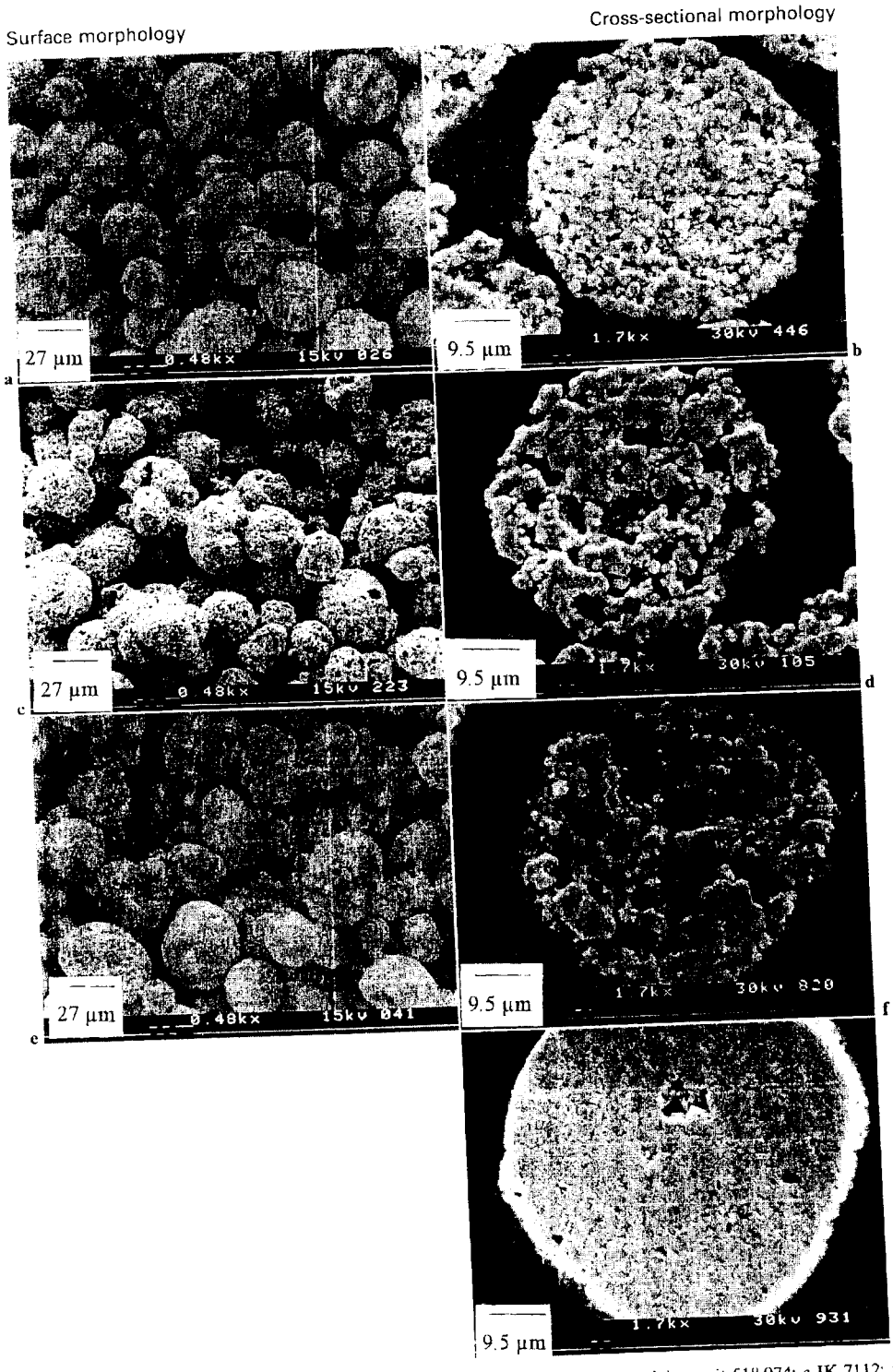

a WC–616; *b* WC–616; *c* Amperit 518.074 (surface morphology of 1341V was similar); *d* Amperit 518.074; *e* JK 7112; *f* JK 7112, dense particles; *g* JK 7112, porous particles

3 Surface morphologies and cross-sections of agglomerated and densified powders

be expected from their generally lower total carbon content. These phases will be carried over into the coating and are generally regarded as detrimental to wear resistance.[19–21] The AI 1101 powder is an exception in this group, since it contains no W_2C. The remaining powders are all similar in phase composition and mostly contain only WC and Co, with the exception of 1341P and JK 7112.

Carbide phase volume fraction

The carbide volume fraction, as determined by the two methods described above, is given in Table 4. The calculated carbide volume percentage is similar for all of the powders and lies between 79·8 and 82·2%. The graphically measured percentages vary widely and are affected by many factors, as already mentioned above. This method, therefore, can not be used with confidence.

Table 5 Percentage phase compositions of powders evaluated in present study

Powder	WC	W_2C	Others	Co (fcc)
Cast and crushed				
Diamalloy 2003	100	84·6	$Co_3W_3C = 7·5$	...
WC-432	100	11·8	$Co_3W_3C = 24·0$	...
			$Co_3W_9C_4 = 3·7$	
AI 1101	100	...	$Co_3W_3C = 4·3$	...
Sintered and crushed				
Diamalloy 2004	100	...	...	1·4
WC-489-1	100	...	...	2·2
AI 1172	100	...	...	< 2·0
1342V	100	...	...	< 2·5
WC-114	100	...	...	1·9
72F NS	100	...	...	1·9
Amperit 516.3	100	...	Co_3W_3C = trace	...
Agglomerated and densified				
WC-616	100	...	...	3·5
1341P	100	1·9	$CoC_x = 3·9$	...
Amperit 518.074	100	...	...	2·6
JK 7112	100	< 1·7	$CoC_x < 2·4$	...

Spray trials and wear tests

The microstructures of the coatings which were produced are described in Table 6 and an example is shown in Fig. 4. Except for the cast and crushed powder, all of the powders produced reasonable coatings, although the degree of WC pullout during polishing was high and the parameters could thus be further optimised. Further work is planned to confirm these results using different spraying parameters.

The cast and crushed powder deposited very badly, a finding which is confirmed by Berget *et al.*[20] and Li *et al.*,[21] who ascribed the lower deposition efficiencies of powders with larger carbide grains to the possible rebounding of the large carbides off the substrate during spraying.[20,21] The abrasion rate of the cast and crushed coating was extremely high, and hence not measurable. The abrasion mass losses of the other three coatings were all identical, at 441–449 g lost after 25 min of testing. When converted to volume losses, using 13·1 g cm^{-3} as the coating density, the coating wear rates were 7% that of an EN3 steel reference sample.

The abrasion rate of the coatings therefore was not affected by whether the powder was sintered and crushed or agglomerated and densified and was also not affected within the sintered and crushed group by whether the carbides were coarse or fine, nor by small differences in the powder particle distribution.

DISCUSSION

The cast and crushed powder coating performed very badly in abrasion tests. It is also the coating for which the starting powder contained high proportions of W_2C and Co_3W_3C. A high proportion of W_2C in the starting powder generally leads to a higher degree of non-WC phases[21] and hence lower wear resistance.

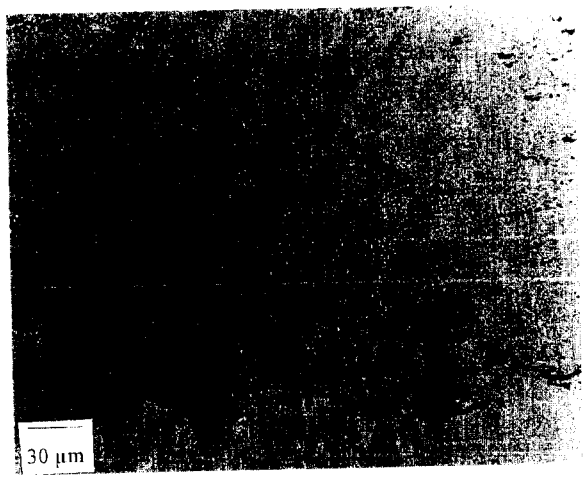

4 Micrograph of coating produced with WC–489–1 powder

The other two powder manufacturing routes did not differ significantly from one another as regards the abrasion resistance of the coatings. This result differs from that of Khan *et al.*,[19] who conducted abrasion tests, similar to those described here, on WC–17Co coatings. They found that HVOF coatings produced using agglomerated powder contained more amorphous phases and had lower wear resistance than coatings produced using sintered and crushed powders. They ascribed this to the greater degree of chemical reaction of the WC with oxygen and with the binder, during spraying of the agglomerated powder, since the open porosity of that powder was much higher.

The most likely explanation for these seemingly conflicting results is that in the present study, a much denser agglomerated and sintered powder was used, and the open porosity did not differ appreciably from that observed in the sintered and crushed powder (cf. Figs. 2*b* and 3*b*). Hence, in the present study, both powders can be expected to react in the flame to a similar degree, therefore resulting in similar wear resistance of the coatings.

Furthermore, in the present study a flame with an excess of oxygen relative to the fuel was used, which means that the flame was cooler than the reducing flame used by Khan *et al.*[19] The lower flame temperature could also explain the relatively high degree of WC pullout observed during sample polishing, owing to lack of complete melting of the binder phase.

Table 6 Summarised results of microstructural examination

Powder	Thickness, μm	Microhardness	Remarks
Cast and crushed WC–432	110	Not determined	Bad coating: high porosity/pullout (estimated at 10%) and large pores, WC size 2–12 μm, poor carbide retention (lots of binder phase visible)
Sintered WC 489 1	270	1357 HV0·3	About 3–4% porosity/pullout, WC size 1–4 μm and good carbide retention, but small lamellar cobalt 'islands' visible (*see* Fig. 4)
Sintered 72F NS	300	1204 HV0·3	About 3–4% porosity/pullout, WC size 1–4 μm and good carbide retention, but cobalt 'islands' of widely varying size visible; overall structure slightly worse than that shown in Fig. 4
Agglomerated WC–616	300	1367 HV0·3	High porosity/pullout (about 5%), WC size 1–4 μm, good carbide retention, a few small cobalt 'islands' visible

CONCLUSIONS

Three WC–12Co powder types have been used to produce HPHVOF coatings. The cast and crushed powder deposited badly and produced a coating with very weak abrasion resistance. The other two powder manufacturing routes produced coatings with very similar abrasion resistances.

These results are in agreement with those of other workers,[19–21] who have shown that the degree of decomposition and reaction of the WC during spraying influences the wear resistance of WC–Co coatings and that the initial phase composition of a powder as well as its surface/volume ratio both play a role in the degree of WC decomposition.

REFERENCES

1. M. L. THORPE and H. J. RICHTER: *J. Therm. Spray. Technol.*, 1992, **1**, (2), 161–170.
2. J. WALTER and W. L. RIGGS: 'Thermal spray research and applications (3rd National Thermal Spray Conference)', 729–733; 1991, Materials Park, OH, ASM International.
3. A. KARIMI, C. VERDON, and G. BARBEZAT: *Surf. Coat. Technol.*, 1993, **57**, 81–89.
4. C. VERDON: 'Microstructure et résistance à l'érosion de revêtements WC–M déposés par projection thermique HVOF', PhD thesis No. 1393, École Polytechnique Fédérale de Lausanne (EPFL), Switzerland, 1995.
5. L. E. McCANDLISH, B. H. KEAR, B. K. KIM, and L. W. WU: 'Protective coatings: processing and characterisation', (ed. R. M. Yazici), 113–119; 1990, Warrendale, PA, TMS.
6. J. F. NERZ, B. A. KUSHNER, and A. J. ROTOLICO: *J. Therm. Spray. Technol.*, 1992, **1**, 147–152.
7. C.-J. LI, A. OHMORI, and Y. HARADA: *J. Therm. Spray Technol.*, 1996, **5**, (1), 69–73.
8. J. F. NERZ, B. A. KUSHNER, and A. J. ROTOLICO: *Mater. Sci. Monogr.*, 1991, **67**, 27–36.
9. B. A. DETERING, J. R. KNIBLOE, and T. L. EDDY: 'Thermal spray research and applications (3rd National Thermal Spray Conference)', 27–31; 1991, Materials Park, OH, ASM International.
10. J. R. FINCKE, W. D. SWANK, and D. C. HAGGARD: 'Thermal spray industrial applications (7th National Thermal Spray Conference)', 325–330; 1994, Materials Park, OH, ASM International.
11. C. HEINZELMAIER and K. K. SCHWEITZER: Proc. Thermal Spray Conf. TS90, Essen, Germany, August 1990, DVS, 51–54.
12. G. BARBEZAT, E. MÜLLER, and B. WALSER: *VDI-Berichte*, 1988, **670**, 853–872.
13. J. F. NERZ, B. A. KUSHNER, and A. J. ROTOLICO: 'Protective coatings: processing and characterisation', (ed. R. M. Yazici), 135–143; 1990, Warrendale, PA, TMS.
14. T. P. SLAVIN and J. NERZ: 'Thermal spray research and applications (3rd National Thermal Spray Conference)', 159–165; 1991, Materials Park, OH, ASM International.
15. P. VUORISTO, K. NIEMI, A. MÄKELÄ, and T. MÄNTYLÄ: 'Thermal spray: research, design and applications (National Thermal Spray Conference)', (ed. C. C. Berndt and T. F. Bernecki), 173–178; 1993, Materials Park, OH, ASM International.
16. M. S. A. KHAN and T. W. CLYNE: 'Thermal spray: practical solutions for engineering problems (National Thermal Spray Conference)', (ed. C. C. Berndt), 113–122; 1996, Materials Park, OH, ASM International.
17. W. J. LENLING, M. F. SMITH, and J. A. HENFLING: 'Thermal spray research and applications (3rd National Thermal Spray Conference)', 451–455; 1991, Materials Park, OH, ASM International.
18. H. E. EXNER *et al.*: *Prakt. Metallogr.*, 1993, **30**, 322.
19. M. S. A. KHAN, T. W. CLYNE, and J. H. STURGEON: 'Thermal spray: a united forum for scientific and technological advances (10th National Thermal Spray Conference)', 681–960; 1997, Materials Park, OH, ASM International.
20. J. BERGET, E. BARDAL, and T. ROGNE: 'Thermal spray: a united forum for scientific and technological advances (10th National Thermal Spray Conference)', 783–789; 1997, Materials Park, OH, ASM International.
21. C.-J. LI, A. OHMORI, and Y. HARADA: *J. Mater. Sci.*, 1996, **31**, 785–794.